

Principle of Least Rattling from Strong Time-scale Separation

Pavel Chvykov* and Jeremy England

Physics of Living Systems, Massachusetts Institute of Technology

A great variety of nonequilibrium systems exhibit predictable macroscopic behavior that arises from the interactions of many microscopic degrees of freedom. It is therefore tempting to develop a general analytical framework for explaining such behaviors, as has long since been achieved for the collective phenomena of equilibrium systems. In this work, we show that for active systems with two clearly separated characteristic time-scales, the driven fast dynamics effectively can be replaced with a thermal bath of inhomogeneous temperature that depends on the state of the slow variables. Besides the resulting connection to equilibrium thermodynamics, the emergent multiplicative noise produces a nonergodic drift towards values of slow variables corresponding to a lower effective temperature. We thus point to a general tendency of slow variables in active systems to find regions in their configuration space whereby the fast behavior is tuned to have a more-orderly, or “least-rattling” response to the driving signal. This means that finely-tuned choices of slow variables can become strongly attractive if they result in an ordered matching between the fast dynamics and the drive. After deriving these general results in a Langevin response-field path integral framework, we validate our findings in a toy mechanical model.

I. INTRODUCTION

The term “active matter” describes a diverse class of externally-driven many-particle systems that are fed by energy sources distributed over many microscopic degrees of freedom. Active matter systems have recently attracted intense interest from both experimenters and theorists, particularly as more examples have been discovered where an inverse cascade of energy from microscopic to macroscopic scales gives rise to complex ordered structures and system-scale dynamical patterns. Self-propelled colloidal particles, for example, have been shown to assemble into highly dynamic “living crystal” structures, while motor-driven protein filaments were observed to form large-scale spiral whorls and topological defects [1–3].

In light of the tremendous success that statistical thermodynamics has had in predicting and explaining the properties of many-particle systems at thermal equilibrium, it is tempting to seek a general theoretical approach to handling their far-from-equilibrium “active” counterparts. Progress in this direction, however, has been hard-won. While many general fluctuation theorem-type results in nonequilibrium statistical mechanics have been proven [4–8] (a short review in [9]), they apply to such a wide-range of different types of systems that they have limited predictive power without further constraining assumptions. Meanwhile, theorists have also achieved impressive successes in predicting properties of particular active matter scenarios – for example by extending the symmetry-based framework of

Landau-Ginzburg to formulating dynamics in terms of mesoscopic order parameters. But these models had to be either quite phenomenological [10, 11], or else to exploit specific features of the system of interest to achieve analytical simplification [12, 13], and thus a more general framework is still wanting.

At thermal equilibrium, it is well accepted that systems settle into sub-ensembles of configurations that strike the right balance between lowering energy and increasing internal entropy. It would be very much desirable to generalize this way of thinking to the far-from-equilibrium case in such a way that some of the predictive power of this thermodynamic intuition might be preserved. However, once it is the case that energy is being injected into a system by driving and dissipated by coupling to external reservoirs, we can no longer assume that the probability distribution over states will minimize the equilibrium free energy. In such a case, we may well then ask: is there anything about the thermodynamic properties of the system that can still be used to predict its structure or dynamical behavior?

A promising way forward lies in recognizing an additional commonality in a broad range of many-body nonequilibrium systems: namely, that different degrees of freedom within them frequently undergo motion on multiple, well-separated time-scales. Such separation can occur if a faster set of active particles act as a bath for a heavier, more slowly relaxing set of larger, extended degrees of freedom: for example, in one numerical study, heavy semi-flexible polymers were suspended in a bath of active colloids and were found to take on a sail-like shape and steadily drift around under power of the microscopic activity [14]. But time-scale separation applies to systems far beyond active matter too: for example river flow (fast) eroding its rock bed (slow), or pass-

* pchvykov@mit.edu

ing cars (fast) creating the “washboard effect” on a dirt-road (slow). Alternatively, in many systems we can usefully identify coarse-grained variables, describing global features of the many-body dynamics, that relax more slowly than the coordinates of individual particles. Such order parameters might then be thought of as a set of slowly-varying constraints on the fast dynamics.

The goal of this article is to treat the case of strong time-scale separation analytically in a generic framework, and to derive a useful predictive relation governing the motion of the slow coordinates. Essentially, the scenario of interest is one in which a given choice of values for slow variables acts as a boundary condition on the fast variables, which are allowed to reach a driven, nonequilibrium steady-state that is specific to those boundary conditions. The question then is: what will the dynamics of the slow-variables look like as they are pushed around by the forces exerted on them by the fast-variables?

The new intuition that will emerge in what ensues below might be termed a “principle of least rattling:” by integrating out the fast degrees of freedom in a response-field, path integral formalism, we show that, in addition to the expected lowest order effect from any average net force the fast variables exert on the slow ones, there is additionally an effective temperature experienced by the slow variables that is determined by the degree to which the fast variables both absorb and randomize energy from the drive. This possibility of replacing the non-equilibrium fast dynamics with a thermal bath of spatially inhomogeneous temperature and drag paves the way for applying thermodynamic results within such an out-of-equilibrium context. One particular consequence is that we expect slow variables to move towards regions of lower effective temperature, where the force fluctuations from the fast variables are weaker. Intriguingly, this means that such systems will be attracted to configurations that *either* reduce the influx of energy from the drive, or simply fall into a pattern of dynamical behavior that reduces the variability (rattling) of how this energy is conveyed and dissipated by the fast variables. This principle can be seen as an attempt at generalization of the discussion in [15], where a periodically sheered colloid was observed to self-organize into a particular “quiescent” configuration.

Of course, nonequilibrium systems with time-scale separation have themselves been extensively studied over the last few decades. The most common context where they have come up is in formalizing the concept of a “thermal bath” – explicitly modelling the fast bath degrees of freedom as a Hamiltonian system, and studying their effects on the slow variables. In this way, one can in some cases recover the

effective friction tensor [16], and the corresponding noise term, related by fluctuation-dissipation theorem [17]. There is also extensive literature studying the conditions and effects of deviations from this basic result, which are generally termed “anomalous diffusion” – see e.g., [18]. Within this context, the “slow” degrees of freedom lack their own dynamics, and are considered only as probes of the fast bath. An active development over the last 5 years came in considering the minimal dissipation required from an external agent to slowly move such probes, thus changing the fast dynamics. A geometric interpretation of this bound was presented in [19], and extended to nonequilibrium baths in [20], as well as to reversible external protocols in [21]. Systems where slow variables have their own dynamics under a conservative coupling to the fast bath has not been considered much, with a recent work for a simple harmonic oscillator probe in [22], and more general exploration in [23, 24], where some formal results relating dissipation and forces on the slow variables were derived.

Most of this previous work has relied on the projection operator technique to obtain the reduced Fokker-Planck equations for the slow variables, as in Ch6.4 of [25]. Alternatively, mutli-scale asymptotic analysis, and its implementation with renormalization group techniques in [26] is another tool that has been used, though more so in the dynamical systems community. Our method, on the other hand, is more closely related to Feynman’s influence functional technique for encoding the effect of an environment on a quantum system [27, 28], and can be practically used for a broader class of problems.

In this context, the contribution of this work is two-fold: first, we present a simpler method of integrating out the fast variables using the response-field path integral framework, and second, we consider systems where the slow coordinates not only evolve under a conservative coupling to the fast ones, but also feed back onto the fast dynamics. Understanding this feedback loop – where the fast variables create an effective nonequilibrium bath for the slow ones, while the slow variables affect the steady-state behavior of the fast ones – is the main focus of the present work.

In the section II of this article, we will present the derivation of our main analytical result, which establishes a relationship between force fluctuations in fast driven variables and the resulting effective temperature experienced by the slow variables in a driven system. In section III, we will carry out a numerical analysis of the kicked rotor on a cart – a time-scale separated, damped, driven dynamical system that is ideally suited for demonstrating the predictive power of the “least rattling” framework.

Not only will this analysis draw clear connections to methods of equilibrium statistical physics and show how they generalize in such a nonequilibrium scenario, but it will also underline how “least rattling” helps to explain the non-trivial relationship between dissipation rate and local kinetic stability in driven systems. Finally in section IV we reflect on the broader consequences of this result for understanding active matter systems.

II. ANALYTICAL SLOW DYNAMICS

In this section, we lay out a general formalism for extracting slow dynamics in stochastic systems with strong time-scale separation. We will model “slow” variables x_a and “fast” variables y_i that evolve according to a coupled system of Langevin equations. Our approach will be to integrate out the fast degrees of freedom and develop an effective theory for the dynamics of the slow variables that is controlled by a small number ϵ which quantifies the time-scale separation between fast and slow. As we carry out this integration, we will show that the effects on x_a from the fast steady-state of the y_i variables at leading order in ϵ are an average force and, more subtly, a random force and renormalized drag that are calculated from the two-point correlation function of the forces acting between x_a and y_i . These latter effects are identified as an emergent, position-dependent effective temperature experienced by the slow coordinates.

A. Setup

Though the method we present can be directly extended to other contexts, it is easiest to illustrate by expressing the system dynamics as a first order system:

$$\begin{aligned}\eta \dot{x}_a &= F_a(x_a, y_i, t) + \sqrt{2T\eta} \xi_a \\ \mu \dot{y}_i &= f_i(x_a, y_i, t) + \sqrt{2T\mu} \xi_i\end{aligned}\quad (1)$$

where the noise ξ is the usual Gaussian white noise: $\langle \xi_\alpha(t) \rangle = 0$ and $\langle \xi_\alpha(t) \xi_\beta(s) \rangle = \delta_{\alpha,\beta} \delta(t-s)$. Taking the limit $\mu/\eta \equiv \epsilon \ll 1$ amounts to explicitly separating x_a as slow modes, and y_i as fast ones (a, b, c index the slow configuration space, and i, j, k – the fast one). The natural physical interpretation of this system as overdamped dynamics in a thermal bath of temperature T , with two different damping coefficients μ and η , the noise amplitudes given by Einstein’s relation, and with the forces F_a and f_i will be implied from now on for clarity, but is not at all necessary. With a slight adjustment the system could as well represent underdamped dynamics, such as in the kicked rotor model system we characterize below.

B. Results

The detailed derivation of the effective slow dynamics is relegated to the Appendix. Here we mention only that the key steps in the derivation. First, we rescale time $t \rightarrow \mu t$, making the slow dynamics obey $\dot{x}_a = \epsilon F_a + \sqrt{2T\epsilon} \xi_a$. Second, we express probability of slow trajectories in terms of the Martin-Siggia-Rose path integral (also termed the response-field formalism) [29], and third, we do a cumulant expansion controlled by ϵ :

$$\begin{aligned}P[x(t)] &= \frac{1}{Z_x} \int \mathcal{D}\tilde{x} \left\langle \exp \left[- \int dt \left\{ i\tilde{x}_a (\dot{x}_a - \epsilon F_a(x, y, t)) + \epsilon T \tilde{x}_a^2 \right\} \right] \right\rangle_{y|x(t)} \\ &= \frac{1}{Z_x} \int \mathcal{D}\tilde{x} \exp \left[- \int dt \left\{ i\tilde{x}_a \dot{x}_a + \epsilon T \tilde{x}_a^2 - i\epsilon \tilde{x}_a \langle F_a \rangle_y + \frac{\epsilon^2}{2} \tilde{x}_a \tilde{x}_b \langle F_a, F_b \rangle_y + O[\epsilon^3] \right\} \right].\end{aligned}\quad (2)$$

In the last line, we see that the $O[\epsilon^2]$ term in the expansion, like temperature T , comes in $\propto \tilde{x}^2$, and thus gives a correction to the noise on the slow dynamics – this is the effect that we will focus on throughout the rest of this paper. Doing this more carefully (as shown in the Appendix) the resulting

slow dynamics, which is our main analytical result,

are

$$\gamma_{ab} \star \dot{x}_b = \epsilon \langle F_a \rangle_{y|fix\ x} + \sqrt{2\epsilon D_{ab}} \star \xi_b \quad (3)$$

$$\gamma_{ab}(x) = \delta_{a,b} + \epsilon \int dt' (t - t') \langle i \tilde{y}_i \partial_b f_i |_{t'}, F_a |_{t'} \rangle_{y|fix\ x}$$

$$D_{ab}(x) = T \delta_{a,b} + \frac{\epsilon}{2} \int dt' \langle F_a |_{t'}, F_b |_{t'} \rangle_{y|fix\ x}.$$

where the matrix square root is defined by $B \equiv \sqrt{D} \Leftrightarrow B.B^T = D$. Here \star product stands for either Itô or Stratonovich convention depending on the relative time-scales of relaxation of the one- and two-point functions under the fast dynamics (i.e., whether the time-scale on which $\langle y_i(t), y_j(t+s) \rangle_{y|fix\ x}$ decays to 0 in s is faster than that on which it relaxes to its new value in t after a change of x). In most cases, the two-point correlations will relax faster than the steady-state distribution itself, thus giving the Itô non-anticipating convention – which we will assume from now on. Note that there is also an $O[\epsilon]$ correction of the damping coefficient, which, for a fully conservative (undriven) system, matches the noise correction to preserve Einstein’s relation, as it should (see sec. d). For non-conservative forces, however, this will not be the case, and the ratio of the effective noise to damping amplitudes can be used to define an effective temperature tensor $T_{eff}(x_a) \equiv \gamma^{-1}.D.(\gamma^{-1})^T$, which will generally depend on the slow coordinates – i.e., the noise on slow variables becomes multiplicative.

It might seem surprising that we can, for an arbitrary first order system, replace the fast dynamics with a mere white-noise contribution. Indeed, what if the fast evolution is integrable rather than chaotic, or has a complicated correlation structure? It turns out that all such scenarios are either still in accord with the above result, or are precluded by requiring all ϵ -truncation to be consistent, as we assume here. This requirement could notably be broken if the fluctuations in the fast variables decay slower than exponentially – a scenario that leads to colored noise and anomalous diffusion, but retains much of the general intuition from eq.3. On the other hand, as the averages are all taken over the thermal noise of the heat bath, the result is automatically consistent both for chaotic and for integrable fast dynamics: in the former case, sensitivity to perturbations caused by the bath will channel most of the chaotic dynamics into the stochastic D_{ab} term, while $\langle F_a \rangle$ might often turn out to be zero by symmetry; while in the latter case, $\langle F_a \rangle$ will capture all of the stable fast evolution (as spontaneous symmetry breaking can occur), with the fluctuations D_{ab} coming only from the actual thermal noise $T \delta_{a,b}$. If a transition

between the two regimes is controlled by the slow coordinates, this can cause dramatic variations in the $T_{eff}(x)$ landscape, and thus in the multiplicative noise amplitude.

C. Practical significance

The significance of the above formal result is that to extract the slow dynamics we need not know everything about the fast modes, but only the one- and two-point correlators of the forces F_a under the y_i steady-state at fixed x_a . All other details of the fast dynamics become irrelevant by the same mechanism as for the central limit theorem. This way, strong time-scale separation amounts to the requirement that the fast fluctuations decorrelate faster than dynamical time-scale of slow variables (e.g., due to stochastic noise or chaos), such that their effect on the slow coordinates adds up as i.i.d. random variables. The deterministic part of the fast dynamics then fixes the mean force, and these fluctuations determine the noise correction. Thus, whether the fast dynamics are integrable or chaotic will determine if their effect looks like noise or a mean force from the perspective of x_a – an intuitively obvious result which attains a precise form in our formalism. As we will see below on an explicit example, the quantitative evaluation of the noise correction becomes easy if we can assume thermalization of the drive energy among the fast fluctuations, as in [30] for example. Finally, generalizing this result can be done within the broader framework of renormalization group flow, which could allow extracting the effective slow dynamics, much like it allows finding large scale physics for quantum or statistical fields [31].

One effect of such multiplicative Itô noise in a stochastic process is that the probability distribution evolves over time from localized initial conditions to become increasingly heavy-tailed (e.g., log-normal distributions are typical). The effect can be that while the exact mean of the distribution can remain fixed over time, the median, and any finite ensemble of trajectories, will drift towards the low-noise regions. Some aspects of this ergodicity-breaking phenomenon were discussed in [32]. For us, this is the statement of the “*Principle of Least Rattling:*” *slow variables tend to non-ergodically settle into regions where fast dynamics are least chaotic.* If, as discussed above, fast degrees of freedom have multiple accessible phases controlled by the slow coordinates, then we will have a tendency for the system to end up in the (most) ordered phase at long times.

III. TOY MODEL

To illustrate the above results, we consider a toy model that is designed to be a simplest possible example capturing all the qualitative features we might expect of more general scale-separated driven systems of interest. Specifically, we take a kicked rotor on a cart setup shown in fig.1a. The fast kicked rotor (Chirikov standard map) dynamics here are chosen as the simplest system that can realize both the chaotic and integrable behaviors under different parameter regimes. Essentially, the system is a rigid pendulum that experiences no external forces except for periodic kicks of a uniform force field (as though gravity gets turned on in brief bursts), and is given by the first two lines in eq.4. We modelled the system to be immersed in a thermal bath by adding a small damping and noise (see third line in eq.4), whose effects have been studied in [33, 34]. The point relevant for the following analysis is that when the driving force amplitude (henceforth called “kicking strength”) is large, the rotor dynamics are fully chaotic, but if the kicking strength drops below a critical value ($K \lesssim 5$), periodic orbits appear in the configuration space, and are made globally attractive in the presence of damping, thus quickly making the dynamics integrable (we refer to this phenomenon below as “dynamical regularization”). Thus, by controlling the effective drive strength, it is possible to switch between chaotic and regular regimes of fast dynamics.

We then fasten the pivot of the fast kicked rotor on a slow cart that can slide back and forth in a highly viscous medium, perpendicular to the direction of the kick accelerations (i.e., along the symmetry axis of the rotor dynamics – see fig. 1a). The cart is pulled by the tension in the rod, which depends on the fast dynamics, while the global cart position x can feed back on the fast dynamics by having a kicking field that varies along the cart’s track $K(x)$. This way we have slow variables conservatively coupled to driven fast dynamics, and a feedback loop controlled through the arbitrary form of $K(x)$. Overall, we argue that, while vastly simplified, this model captures essential physical features of many multi-particle nonequilibrium systems of potential interest.

A. Model Setup

The toy model explored here is presented in fig. 1a: the kicked rotor is attached to a massless cart moving on a highly-viscous track, which ensures that cart’s velocity is much smaller than the rotor’s. The exact equations of motion for the system can be derived from a force-balance, and in their dimension-

less form become:

$$\begin{aligned}
 \dot{\theta} &= v \\
 \dot{v} &= -K(x) \sin \theta \delta(t - n) \\
 &\quad - b v + \sqrt{2Tb} \xi - \ddot{x} \cos \theta \\
 c \dot{x} &= -\partial_x U(x) + \underbrace{\sqrt{2Tc} \xi + \sin \theta (v^2 - \ddot{x} \sin \theta)}_{\equiv F_x}
 \end{aligned} \tag{4}$$

where all lengths are measured in units of rotor arm length, time in units of kicking period, and the angle θ is 2π -periodic. Note that for practical reasons (see Supplementary Materials), we also assumed that the cart is momentarily pinned down during each kick, so as to remove the term $\frac{1}{2}K(x) \sin 2\theta \delta(t - n)$ that should otherwise be included in F_x due to the direct coupling of the kicks to the cart. For now, we can motivate this by saying that the interesting problem is where the driving force affects the slow dynamics only by means of the fast ones, and not directly, while this chosen implementation can simply be viewed as an additional component of the drive protocol. Additionally, to provide more modelling freedom, we can include an arbitrary potential $U(x)$ acting directly on the cart to produce a conservative force. Time-scale separation in this model implies that back reaction from cart dynamics on the rotor is small – i.e., here that $\ddot{x} \ll K$ (by differentiating the last line, we see that indeed $\ddot{x} \sim O[v^3/c] \ll 1$ for $c \gg 1$). Thus the leading-order feedback from the slow variables onto fast dynamics comes from x -dependence of K , which we have full control over, making for a convenient toy-model. We also independently assume that $b \ll 1$ so that fast dynamics are close to the ideal kicked rotor and retain its features.

B. Analytical Evaluation

For large K (above the dynamical regularization threshold, i.e. $K \gtrsim 5$), the steady-state of the fast dynamics is fully chaotic, and thus thermal – i.e., we assume thermalization of the entirety of drive energy among the fast fluctuations, as happens in [30] for example. This way, the steady-state distribution is Boltzmann, which is here uniform over θ and Gaussian over v . The symmetry of this state over θ and v gives $\langle F_x \rangle_{s.s.} = 0$, making the fluctuations dominant. The only remaining parameter we need to find – the amplitude of v -fluctuations, or rotor temperature T_R – is constrained by energy balance. In general, to keep an ergodic system at an effective temperature that is higher than that of its

bath requires dissipation [35]:

$$\begin{aligned}\delta Q &= \int dt v \circ (bv - \sqrt{2T_0} b \xi) = b (\langle v^2 \rangle - T_0) \delta t \\ \mathcal{P} &\equiv \frac{\partial Q}{\partial t} = b (T_{eff} - T_0).\end{aligned}\quad (5)$$

(for 1D systems with mass=1). Moreover, we can find the power exerted by the kicking force to be $\mathcal{P} = K^2/4$ in the chaotic regime, which in the steady-state must balance the dissipated power. This allows us to extract the effective rotor temperature: $T_R \sim T_0 + \frac{K^2}{4b} + O[\frac{1}{c}]$ (see Supplementary Material for details).

This, however, only gives us information about the fast behavior, while the x -noise correction that we want will also depend on the nature of the rotor-cart coupling. This way, we need to evaluate the x -force correlations and $\delta T_x = \frac{1}{2c} \int dt \langle F_x(t), F_x(s) \rangle$, where as above, $F_x = v^2 \sin \theta - \ddot{x} \sin^2 \theta =$ (centripetal F_c) - (inertia F_i) is the force on the cart. The calculation is relatively straightforward and detailed in the Supplementary Material, where we also show that γ damping-coefficient correction is 0 by symmetry of the (θ, v) distribution. We find that, while the inertial term can be ignored at leading order, the correlations of the centripetal force give us $\delta T_x = \frac{1}{2c} \int dt \langle F_c, F_c \rangle = K^2/16c$. Note here that this multiplicative noise correction should be interpreted in the Itô sense, as the $\langle F_c, F_c \rangle$ correlations decay on a time-scale faster than kick-period (see Appendix, b).

For $K \lesssim 5$, on the other hand, the rotor moves periodically in one of the regular attractors. This means that the cart experiences no additional stochasticity other than that from the thermal bath, but as some of these attractors spontaneously break the left-right symmetry of the problem, we get $\langle F_x \rangle_{s.s.} \neq 0$. As the motion in most of these attractors is very simple - $n \in \mathbb{Z}$ full revolutions of the rotor per kick - we can estimate this force explicitly: $\langle F_x \rangle_{ss} = \int_0^1 dt v^2(t) \sin \theta(t) \sim b v_n + v_n^3/2c$, where $v_n \equiv 2\pi n$, and $\theta(t)$ and $v(t)$ were estimated by integrating the equations of motion 4 at leading order (see Supplementary Materials).

Compiling the resulting predictions for the cart motion, we get:

$$\begin{aligned}c \dot{x} &= -\partial_x U(x) + \langle F \rangle + \sqrt{2c T_{eff}} \cdot \xi \quad (6) \\ \langle F \rangle &= \begin{cases} v_n (b + v_n^2/2c) & K \lesssim 5 \\ 0 & K \gtrsim 5 \end{cases} \\ T_{eff} &= \begin{cases} T_0 & \\ T_0 + K^2/16c & \end{cases}\end{aligned}$$

with $v_n \equiv 2\pi n$ and n some random integer, typically smaller than $O[\sqrt{T_R}]$. Another quantity we can easily estimate for the two phases is the energy dissipation rate:

$$\dot{Q} = \begin{cases} v_n^2 (b + v_n^2/2c) & K \lesssim 5 \\ K^2/4 & K \gtrsim 5 \end{cases} \quad (7)$$

Numerical simulations confirm these predictions in fig.1 c, d, and e respectively.

C. Numerical Tests

To verify the above analytical results, we can run numerical simulations of the full system dynamics in eq. 4. To begin, we check the cart dynamics for different values of (x -independent) K (and $U(x) = 0$). Fig. 1b shows typical cart trajectories for K in the regular and chaotic regimes. More systematically, plotting the apparent average drift $\langle F \rangle$ and fluctuations T_{eff} for multiple realizations at each K , we get plots in c and d of fig. 1 respectively. We thus see quantitative agreement between the prominent features of these plots and the results of eq. 6 - shown here as black lines. Finally fig. 1e shows the heat dissipation rate in the different possible steady-states, showing that while lowering T_{eff} corresponds to decreased dissipation within the chaotic phase, this rule is violated if we enter a regular dynamic attractor.

Note that as the original problem is stated exactly, and our method allows for full analytical treatment of the slow variables, there are no fitting parameters in any of the curves we are comparing against throughout the numerical study. We use $c = 5 \times 10^4$, $b = 0.1$ for all simulations, and to emphasize the effects from fluctuations of the fast variables, we take the actual thermal bath to be at a vanishingly low temperature $T_0 \sim 0$, unless otherwise stated.

While fig. 1 shows agreement of one- and two-point functions of cart position with our analytical prediction, we have yet to check that the fast dynamics can really be approximated by an effective thermal bath. One convincing way to do this is to introduce a non-trivial potential landscape $U(x)$ acting on the cart's position x , and check the resulting steady-state distribution $p(x)$ against Boltzmann statistics at the predicted temperature T_{eff} . Figure 2a shows the agreement between the histogram produced by this simulation and the curve for the expected Boltzmann distribution.

To see that the $T_{eff}(x)$ landscape remains the appropriate description even for non-uniform $K(x)$, we can calculate the steady-state distribution in a $K(x)$

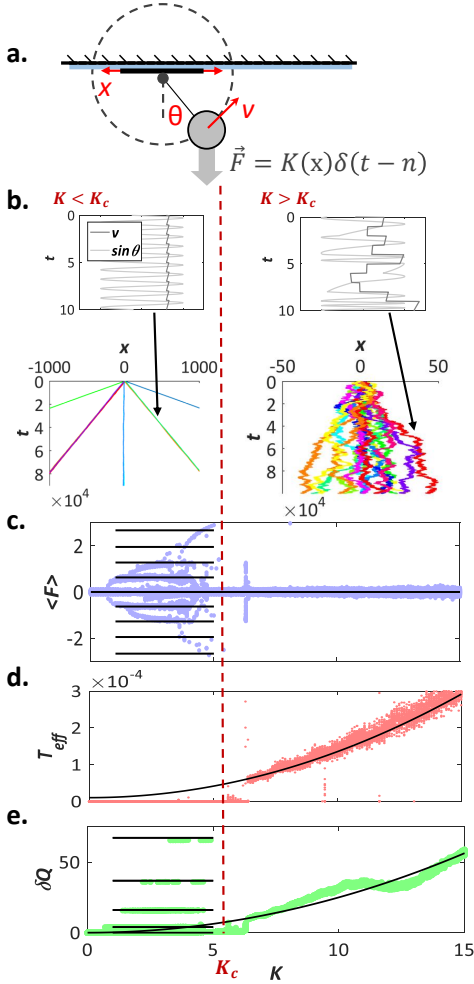


FIG. 1: a. schematic of the kicked-rotor-on-a-cart toy model. b. numerical realizations of typical cart trajectories over time for driving force below ($K = 3$: regular / ordered regime) and above ($K = 8$: chaotic regime) the ordering transition (at $K_c \sim 5$), along with samples of the corresponding fast (θ, v) dynamics. c,d,e. average force, fluctuations, and dissipation rates in the cart dynamics, measured from trajectories as in panel (b), for the various values of K , along with analytical predictions (in black) from eq.6

landscape, now letting $U(x) = 0$. The expected distribution for free diffusion in a temperature landscape can easily be found using, e.g., Fokker-Planck equation, and gives $p(x) \propto 1/T(x)$. This is well confirmed by simulations in fig. 2b, thus showing that at least in the steady-state, probability density does indeed collect in low-temperature regions.

The last natural test that we mention here is to see how $T_{eff}(x)$ landscape can counteract the forces of

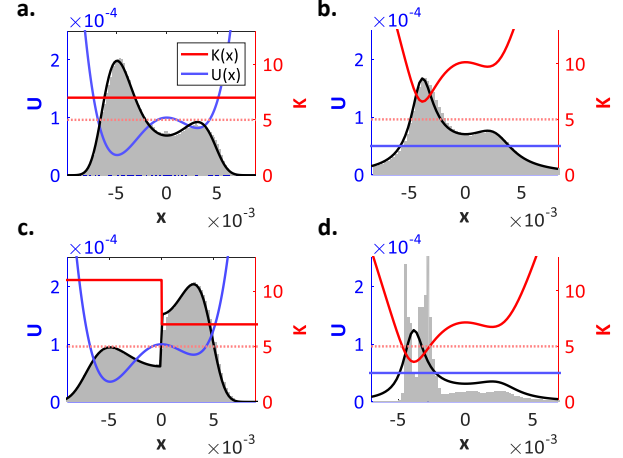


FIG. 2: Histograms (grey) of the steady-state cart positions in simulation with: a. constant $K(x) = K$ and in a potential landscape $U(x)$ plotted in blue (black curve gives the expected Boltzmann distribution); b. $U(x) = const$ and $K(x)$ landscape in red (black curve shows $1/T_{eff}(x)$ – solution of the Fokker-Planck equation) c. $U(x)$ as in a. and $K(x)$ step-function (analytical prediction plotted in black is given by eq.8). d. $U(x) = const$ and $K(x)$ as in b., but shifted down to dip below the critical $K_c \sim 5$ value – dotted red line (black curve again shows $1/T_{eff}(x)$ outside of ordered region) – this shows that probability gets localized at the two transition points at long times.

$U(x)$ – specifically changing the stability in a double-well potential. This setup is shown in 2c, where the higher-energy potential well is stabilized by having a lower T_{eff} . The numerical result is correctly predicted by the steady-state solution of the Fokker-Planck equation with the expected effective temperatures in each well (labels L and R denote left and right wells respectively), as shown in fig. 2c:

$$p(x) = \frac{1}{Z} \begin{cases} \frac{1}{T_L} e^{-U(x)/T_L} & x < 0 \quad (L) \\ \frac{1}{T_R} e^{-U(x)/T_R + \Delta} & x > 0 \quad (R) \end{cases} \quad (8)$$

$$\Delta \equiv U(0) \left(\frac{1}{T_R} - \frac{1}{T_L} \right)$$

In the limit of a discrete jump process between the two wells (wells with equal internal entropy separated by a high barrier), this exact solution becomes well approximated by that obtained from current-matching with the expected jump rates: $r_{\rightarrow} = e^{-(U(0)-U_L)/T_L}$ and $r_{\leftarrow} = e^{-(U(0)-U_R)/T_R}$. The key non-equilibrium feature in these solutions is the dependence of the probabilities in either well on the barrier height $U(0)$ via Δ – for higher barriers

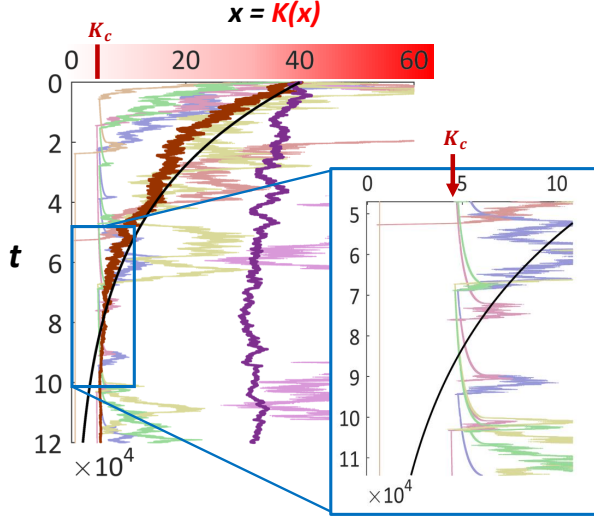


FIG. 3: Typical cart trajectories in linear $K(x)$ landscape ($U(x) = \text{const}$) all starting from one point, along with their mean (purple) and median (brown). Black curve shows the analytical prediction for the median, while mean is expected to be constant at small times. Inset shows the regularization transition at $K_c \sim 5$, where effective temperature drops abruptly to 0, and median departs from the smooth decay. x -axis is labelled in units of K

the temperature difference becomes more important. This example gives the first non-trivial application of thermodynamic intuition from $T_{eff}(x)$ landscape to solution of our non-equilibrium system. Projecting this concept onto a broader context, we note that this setup is a particular realization in the class of problems of iterative annealing (e.g., used in chaperoned protein folding [36], etc).

D. Least rattling

Having confirmed the steady-state and thermal properties of the slow behaviors, we next want to look at the predictive power of our formalism for transient behaviors and currents, again in the presence of inhomogeneous fast dynamics. The first example we consider is transient cart motion in linearly varying $K(x) = \kappa x$. The simulation results are shown in fig. 3. As mentioned above, free diffusion in a temperature gradient results in a median drift to low T , as observed here. Explicitly, the slow dynamics in this case $c\dot{x} = \frac{\kappa}{2\sqrt{2}}x \cdot \xi$ can be solved exactly to give $\ln x(t) = -\left(\frac{\kappa}{4c}\right)^2 t + \frac{\kappa}{2\sqrt{2}} \mathcal{N}(0, t)$ (with \mathcal{N} giving the normal distribution with variance t),

from which we can read off the mean $x(t) = x_0$ and median $x = x_0 \exp\left[-t(\kappa/4c)^2\right]$ behaviors. The latter is plotted in black in fig.3 and well reproduces the simulation result in brown. Note that for any finite ensemble of trajectories, or for a bounded system, the mean will eventually go to low temperatures as well, but not as cleanly or predictably – so the constant mean value is not practically realizable at long times. The inset focuses on the crossover into regular dynamics, where we see that the symmetry-broken drift-force $\langle F_x \rangle$ can either take the cart to the $K = 0$ absorbing state (as detailed in the further inset), or back out into the chaotic regime. In the latter case, the cart typically diffuses back down to the transition again. The resulting oscillations cause a (transient) accumulation of probability around the critical point, giving a peculiar realization of self-organized criticality. This critical region itself is also interesting as the correlations of the fast variables persist for long times, and can thus break the time-scale separation assumption – but this will have little effect on the global system behavior. The overall takeaway here is the emergent “least rattling:” slow dynamics drift towards regions where fast ones are less stochastic.

To further illustrate the importance of the regularization transition on the slow dynamics, we consider the probability distribution $p(x)$ in the presence of $K(x)$ landscape (and no potential $U = 0$), as in fig. 2b., but shifted down such that it dips slightly below the regularization transition at its lowest point – fig. 2d. The resulting small zero-temperature region in x , corresponding to integrable fast dynamics, becomes absorbing, collecting most of the probability density over time (see fig. 2d). Note again that probability accumulates at the critical transition points, giving the two-pronged shape. We stress here the observed sharp localization transition of the steady-state distribution as soon as some regular regime of the fast dynamics becomes accessible – i.e., the slow variables find the regularized region even if it requires some fine-tuning. (This trade-off between least-rattling and entropic forces can be made quantitative.)

E. Anomalous diffusion

The last example we present shows that besides an effective temperature landscape, the regular dynamical phase accessible to this model can give rise to apparent anomalous diffusion. To begin, Fig. 4a shows an implementation of Buttiker-Landauer ratchet using our model: periodic $U(x)$ and $K(x)$ landscapes, with a relative phase-offset of $\pi/2$ create a steady-state current being pumped, in this case to

the right. Intuitively, this happens because a higher effective temperature in the right half of the potential well makes it easier for the cart to overcome the right potential barrier than the left one. The interesting behavior appears when we shift the $K(x)$ wave downward to straddle the transition point at $K \sim 5$ (fig. 4b). In this case the pumped current reverses direction and becomes an order of magnitude *larger* – even if we reduce the amplitude of the $K(x)$ variation. To understand this, it helps to look at some typical realizations of barrier-crossing trajectories at the bottom of fig. 4. While in panel a. transitions are achieved by stochastic fluctuations that are exponentially suppressed by the Boltzmann factor, in panel b., these are achieved by a directed symmetry-broken drift force $\langle F \rangle > \partial_x U$, and thus the crossing probability is just the probability of the fast dynamics finding the appropriate regular attractors. These ballistic-like trajectories of the cart in the regular regime can be usefully thought of as anomalous super-diffusion with exponent $\alpha = 2$. Also, in so far as the barrier crossing becomes easier as we lower $K(x)$ through the critical value, we can say that the diffusion becomes stronger, thus showing non-monotonicity with K – reminiscent of the findings in [37].

IV. DISCUSSION

The equilibrium partition function that is computed for the Boltzmann distribution is a powerful formal tool for making predictive calculations in thermally fluctuating systems. Its success stems from two key simplifying assumptions: first, that energy only enters or leaves the system of interest in the form of heat exchanged at a single temperature, and second, that the system and surrounding heat bath uniformly sample joint states of constant energy. This latter ergodic assumption essentially amounts to eliminating time from the picture, so that energy and probability become interchangeable.

The nonequilibrium scenario is generally less tractable than its equilibrium counterpart both because time has not been eliminated from our description of the system, and also because energy is permitted to enter and leave the system via different couplings to the external environment. Thus, the specific approach to modelling some nonequilibrium systems we have described here seeks to recover some of the desirable advantages of the equilibrium description by exploiting time-scale separation in two ways: first, by only allowing nonequilibrium drives to couple to a fast subset of variables, and second, by “partially removing” time from the picture by replacing the fast variables with a timeless thermal

bath approximation. This “conveys” the entire time-dependence of the problem into the resulting effective slow dynamics.

Adopting such an approach by no means recovers the simplicity of the equilibrium picture, however, it does give rise to a relatively tractable effective description of the dynamics. As we have seen, slow variables in such a scenario experience not only a mean force landscape from the steady-state of the fast variables, but also are expected to drift in the direction of decreasing fictitious temperature set by the fast variable force fluctuations. Crucially, the latter effect is non-ergodic, thus somehow capturing the breaking of ergodicity typical of driven dynamics in a simple and tractable picture.

We have established that this effective picture is quantitatively predictive of the diffusive and stationary behavior of distributions for such slow variables in a simple rotor-on-cart toy model. The tendency of such systems to gravitate to values of slow variables that reduce the effective temperature of fast ones suggests a interesting relationship between dissipation and kinetic stability in driven systems. Although nonequilibrium steady-states are not in general required to be extrema of the average dissipation rate, it is true that the minimum required dissipation to maintain an effective temperature scales with T_{eff} . Accordingly, there may be a subset of systems where the drift to lower effective temperature is indeed accompanied by a drop in dissipation. However, for cases where dissipation instead goes to maintaining dynamically regular motions, steady-state behavior might be dominated by a highly dissipative, stable attractor of low T_{eff} .

Moreover, if fast variables can undergo a dynamical ordering transition that is controlled by the slow coordinates, the corresponding drop in effective temperature can be dramatic. As such, this case opens up the intriguing possibility that dynamical ordering in fast variables might serve as a mechanism for the long-term kinetic stability for slow variables. Moreover, if dynamical ordering only can occur for rare, finely-tuned choices of slow variables, this stability could appear as a tendency toward self-organized fine-tuning in the slow-variable dynamics.

Accordingly, we suggest that an interesting future set of applications for the least rattling approach may lie in the active matter setting, where it is frequently the case that coarse-grained macroscopic features of active particle mixtures relax more slowly than the strongly driven microscopic components. The diversity of self-organized collective behaviors exhibited by such systems is well-known, and it may be useful to characterize these behaviors in terms of their possibly fine-tuned relationships to driven force fluctuations on the microscopic level. Future work

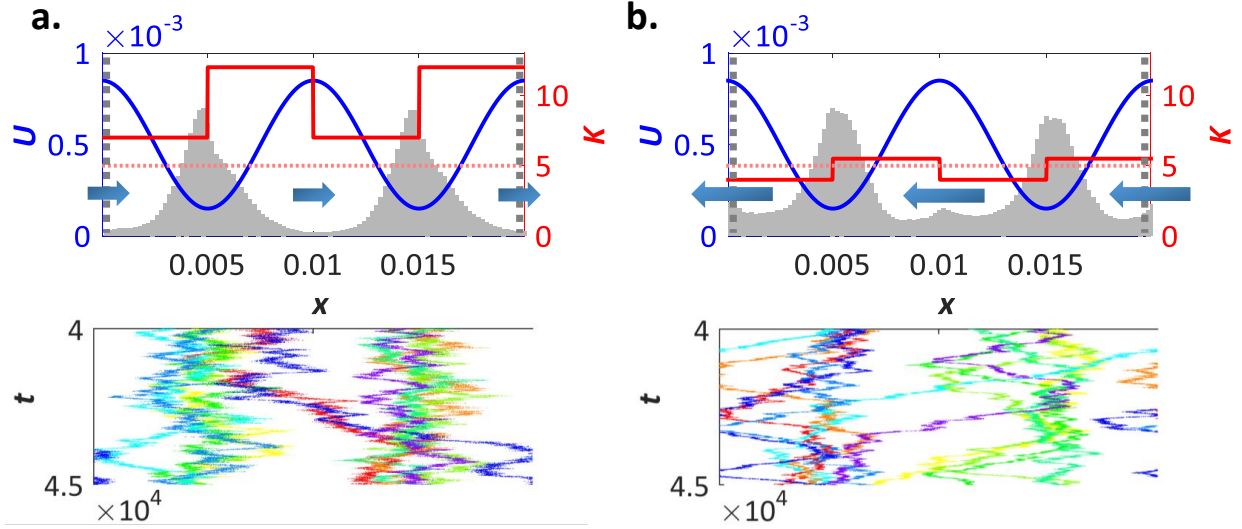


FIG. 4: Simulated steady-state cart-position distributions for the shown $U(x)$ (blue) and $K(x)$ (red) landscapes (x is periodic). These result in a pumped steady-state current (block arrows), with the typical barrier-crossing trajectories shown at the bottom. Unlike in all the above simulations, thermal bath temperature $T_0 = 10^{-4} > 0$ was taken in these to smooth out the critical behavior. Straddling the critical point with $K(x)$ in panel b produces a ten-fold larger (and reversed) current, even for smaller absolute variation in $K(x)$

must focus on generalizing our current approach to modelling the dynamics of such coarse-grained variables.

Appendix : Derivation of Effective slow dynamics

Starting with the explicitly time-scale separated dynamics given by the system 1, the first step is to explicitly bring our small parameter $\epsilon \equiv \mu/\eta \ll 1$ into the equations by rescaling time $t \rightarrow \mu t$, which gives:

$$\begin{aligned} \dot{x}_a &= \epsilon F_a(x_a, y_i, t) + \sqrt{2\epsilon T} \xi_a \\ \dot{y}_i &= f_i(x_a, y_i, t) + \sqrt{2T} \xi_i \end{aligned} \quad (\text{A.1})$$

This will allow us to do a systematic expansion in ϵ below. For later convenience, let us explicitly introduce the time-scales of slow $\tau_S \sim O[1/\epsilon]$ and fast $\tau_F \sim O[1]$ relaxation. Next we want to integrate out the fast degrees of freedom y_i , which we can explicitly do by writing down the Martin-Siggia-Rose (MSR) path integral expression for the probability of a particular slow trajectory $x_a(t)$, as given in the first line of eq. 2. For clarity of notation, we have represented the full path-integration over the fast dynamics as the average:

$$\langle \mathcal{O} \rangle_{y|x(t)} \equiv \frac{1}{Z_y[x(t)]} \int \mathcal{D}y \mathcal{D}\tilde{y} \mathcal{O} \exp \left[- \int dt \{ i\tilde{y}_i (\dot{y}_i - f_i(x(t), y, t)) + T \tilde{y}_i^2 \} \right] \quad (\text{A.2})$$

Note that so far, this is defined for a specific fixed slow trajectory $x(t)$. With this notation set, we now observe that the only y -dependence that the average can act on in eq. 2 is that in $F(x, y, t)$. Thus, all the

other terms can be taken out of the average, while the remaining small ϵF_a exponent can be treated with a cumulant expansion:

$$\begin{aligned} & \left\langle \exp \left[i \epsilon \int dt \tilde{x}_a F_a(x, y, t) \right] \right\rangle_{y|x(t)} = \\ & \exp \left[i \epsilon \int dt \tilde{x}_a(t) \langle F_a(x, y, t) \rangle_{y|x(t)} - \epsilon^2 \int dt \int dt' \tilde{x}_a(t) \tilde{x}_b(t') \langle F_a(x, y, t), F_b(x, y, t') \rangle_{y|x(t)} + O[\epsilon^3] \right] \end{aligned} \quad (\text{A.3})$$

As this is the only part of the path integral in eq 2 that carries the coupling to fast dynamics, it will source all the interesting emergent effects (i.e., coupling renormalizations) for the slow modes, and we thus focus on this for most of this Appendix.

a. Averages over fast dynamics

Before getting into the physical implications of the different terms in the expansion, let's discuss how to go about calculating the averages $\langle \mathcal{O} \rangle_{y|x(t)}$. Indeed, as defined in eq. A.2, these averages are just short-hand for path integrals over the full fast dynamics in the presence of arbitrarily time-varying

slow variables $x_a(t)$, and hence at this point, merely formal, but not very informative, quantities. On the other hand, intuitively we know that at the lowest order in ϵ , these averages should reduce to averages over the y -steady states under fixed x : $p_{ss}(y|x)$. To derive this result as well as the first correction in ϵ , we need to once again develop a systematic expansion. Besides \mathcal{O} (see below), the only dependence on the trajectory $x(t)$ in eq A.2 comes in through the force f_i (and similarly in the partition function), which by time-scale separation assumption, we know will vary only slightly on the fast time-scale τ_F : $f_i(x(t), y, t) = f_i(x(t_0), y, t) + (t - t_0) \dot{x}_a(t_0) \partial_a f_i(x(t_0), y, t) + O[\epsilon^2]$. Plugging this expansion into eq. A.2 and Taylor expanding both numerator and denominator (normalization Z_y) in ϵ , we get:

$$\begin{aligned} \langle \mathcal{O} \rangle_{y|x(t)} &= \langle \mathcal{O} \rangle_{y|x(t_0)} + \left\langle \mathcal{O}, \int dt i \tilde{y}_i (t - t_0) \dot{x}_a(t_0) \partial_a f_i(x(t_0), y, t) \right\rangle_{y|x(t_0)} + O[\epsilon^2] \\ &= \langle \mathcal{O} \rangle_{y|x(t_0)} + \dot{x}_a(t_0) \int dt (t - t_0) \langle \mathcal{O}, i \tilde{y}_i \partial_a f_i |_{t'} \rangle_{y|x(t_0)} + O[\epsilon^2] \end{aligned} \quad (\text{A.4})$$

The averages here $\langle \mathcal{O} \rangle_{y|x(t_0)}$ are at a fixed x , and thus are precisely the averages over y steady-states $p_{ss}(y|x(t_0))$. Note also that at this order, the possible x -dependence of \mathcal{O} is accounted for at the slow time-scale and does not give any additional contributions here. At the next order in ϵ , however, the variations of \mathcal{O} and f_i on the relaxation time-scale

τ_F begin to interact, giving new contributions. Generally, Feynman diagrams are the only practical way to go to higher orders as the number of correction terms potentially becomes large. We do not employ diagrams here because they are not practical for the general context we are working with – but they do become very useful in specific examples.

Applying the result in eq. A.4 to our cumulant expansion A.3, we get

$$\langle F_a(x, y, t) \rangle_{y|x(t)} = \langle F_a |_{t'} \rangle_{y|f_{ix} x(t)} - \dot{x}_b(t) \int dt' (t - t') \langle i \tilde{y}_i \partial_b f_i |_{t'}, F_a |_{t'} \rangle_{y|f_{ix} x(t)} + O[\epsilon^2] \quad (\text{A.5})$$

Remembering the form of eq. 2, we recognize the

correction term here as a correction (or renormal-

ization) of the damping coefficient of the original slow dynamics. Crucially, this correction comes in at the same order in ϵ as the $O[\epsilon^2]$ term in eq. A.3, and must thus be kept in our expansion. By the same token, the equivalent correction of the $\langle F_a(t), F_b(t') \rangle_{y|fix\ x(t)}$ term only comes in at a higher order and is thus ignored at this stage. Nonetheless, it is interesting to note that including higher order corrections would also introduce an inertia-like term into our slow dynamics (mass renormalization, $\propto \ddot{x}$), as discussed in [22]), as well as higher derivative at progressively higher orders.

b. Noise correction

The key thing to note from the above results is that at $O[\epsilon^2]$, the only thing we need to compute the slow dynamics are the one- and two-point functions of the various variables in the y -steady-states. Thus we need neither the full form of the steady-state distribution of the fast variables, nor the deviations from this steady-state under dynamic $x(t)$. This result should be thought of as (and really is a form of) the central limit theorem.

Now that we have a sense of what the different terms in the cumulant expansion A.3 mean mathematically, we can turn to their physical implica-

tions. We already mentioned the correction of the x -damping coefficient that we get by resolving the $\langle F_a \rangle_{y|x(t)}$ term in terms of y -steady-states. The only other contribution at this same order is the second term in the expansion A.3. This will contribute an additional noise term to the resulting slow dynamics, as it will enter the path integral along with T , correcting the \tilde{x}^2 operator. However, this noise term would only be white if $\langle F_a(t), F_b(t') \rangle_y \sim \delta(t - t')$, which in general need not be the case, hence making the noise correction colored. Intuitively, we see that because of time-scale separation, y fluctuations will decorrelate much faster ($\delta t \sim O[1]$) than the slow time-scale we are sampling by observing x ($\tau_S \sim O[1/\epsilon]$). This makes the short-range correlations of the noise correction unimportant for the slow evolution, allowing us to approximate it by white noise.

More formally, this situation is precisely identical to having a UV cutoff in a field theory given by, e.g., finite lattice spacing. Similarly, taking the white-noise approximation here corresponds to sending such a cutoff to infinity, which is justified as long as all our observables are confined to energy-scales (or here time-scales) far lower than said cutoff. Explicitly, the approximation we are making (which formally comes from the assumption of RG universality in the fast dynamics):

$$\int dt \int dt' \tilde{x}_a(t) \tilde{x}_b(t') \langle F_a(x, y, t), F_b(x, y, t') \rangle_{y|x(t)} \approx \int dt \tilde{x}_a(t) \tilde{x}_b(t) \int dt' \langle F_a(x, y, t), F_b(x, y, t') \rangle_{y|fix\ \hat{x}} \quad (\text{A.6})$$

One reason why we must be careful in taking this white-noise limit is that the precise limiting procedure will determine whether the correct interpretation of the resulting multiplicative white noise is Itô or Stratonovich, resulting in observable consequences on the slow time-scale. This question is related to the choice of \hat{x} where to evaluate the y -steady-state in the RHS of eq. A.6, as well as, independently, where to evaluate the explicit dependence $F_a(x)$. To avoid very messy notation, we assume away the latter point by restricting the form of $F_a(x, y, t) = \tilde{F}_a(x) + F_a(y, t)$, which then makes the above expression A.6 depend on x only via the steady-state $p_{ss}(y|\hat{x})$ (\tilde{F} drops out altogether): define $\delta T(\hat{x}) \equiv \frac{\epsilon}{2} \int dt' \langle F_a(y, t), F_b(y, t') \rangle_{y|fix\ \hat{x}}$. Again, this restriction is not necessary and is taken here for convenience.

Thus, we see that if we discretely change \hat{x} , two separate time-scales (both fast, $\sim O[1]$) control the

relaxation of $\delta T(\hat{x})$: τ_F , on which $p_{ss}(y|\hat{x})$ globally relaxes to its new form (i.e., relaxation time of one-point functions), and τ_{F2} , on which the two-point function $\langle F_a(y, t), F_b(y, t') \rangle_{y|fix\ \hat{x}}$ decays. If $\tau_F \ll \tau_{F2}$, then we have the usual result that the white-noise limit of multiplicative colored noise should be interpreted as Stratonovich (see Ch.6.5 in [25]). On the other hand, for $\tau_F \gg \tau_{F2}$ we see that $p_{ss}(y|\hat{x})$ remains essentially fixed while the noise correlations decay, and so the noise amplitude must be evaluated according to the value of x at the beginning of the τ_{F2} interval, i.e., in non-anticipating Itô convention. Note that while both limits are possible, the latter is typical, especially for many-body systems, since the relaxation of $p_{ss}(y|\hat{x})$ proceed via relaxations of two-point functions throughout the system. Finally, note that the same Itô / Stratonovich ambiguity occurs in the expression for the damping correction A.5 and is resolved in exactly the same way as here.

c. *Compiling results*

Finally, we are in a position to put everything together. We use our final expressions for damping A.5 ($\delta\gamma_{ab}(x) \equiv \int dt' \langle i \tilde{y}_i \partial_b f_i |_{t'}, F_a |_t \rangle_{y|fix x(t)}$), and noise correc-

tion A.6 ($\delta T(\hat{x}) \equiv \frac{\epsilon}{2} \int dt' \langle F_a(y, t), F_b(y, t') \rangle_{y|fix \hat{x}}$) in the cumulant expansion A.3, and plug that into the full expression for the probability distribution over slow paths 2 to get:

$$P[x(t)] = \frac{1}{Z_x} \int \mathcal{D}\tilde{x} \exp \left[- \int dt \left\{ i \tilde{x}_a \dot{x}_a + \epsilon T \tilde{x}_a^2 - i \epsilon \tilde{x}_a \left(\langle F_a \rangle_y - \delta\gamma_{ab} \star \dot{x}_b \right) + \tilde{x}_a \delta T_{ab} \tilde{x}_b + O[\epsilon^3] \right\} \right]$$

$$= \frac{1}{Z_x} \int \mathcal{D}\tilde{x} \exp \left[- \int dt \left\{ i \tilde{x}_a \left(\gamma_{ab}(x, t) \star \dot{x}_b - \epsilon \langle F_a \rangle_y \right) + \epsilon \tilde{x}_a \star D_{ab}(x, t) \star \tilde{x}_b + O[\epsilon^3] \right\} \right].$$

where

$$\gamma_{ab}(x, t) \equiv \delta_{a,b} + \epsilon \int dt' (t - t') \langle i \tilde{y}_i \partial_b f_i |_{t'}, F_a |_t \rangle_{y|fix x}$$

$$D_{ab}(x, t) \equiv T \delta_{a,b} + \frac{\epsilon}{2} \int dt' \langle F_a |_{t'}, F_b |_t \rangle_{y|fix x}$$

The resulting path integral can then be used to extract the corresponding Langevin equation for the slow dynamics:

$$\gamma_{ab}(x) \star \dot{x}_b = \epsilon \langle F_a \rangle_{y|fix x} + \sqrt{2\epsilon D(x)_{ab}} \star \xi_b \quad (It\hat{o})$$

$$\star \equiv \begin{cases} \cdot & [It\hat{o}] & \tau_{F2} \ll \tau_F \\ \circ & [Strat] & \tau_{F2} \gg \tau_F \end{cases}$$

where ξ_a is the usual white noise: $\langle \xi_a(t), \xi_b(t') \rangle = \delta_{ab} \delta(t - t')$, and the square root of the matrix D_{ab} is defined by the condition $\sqrt{D} \cdot \sqrt{D}^T = D$. Finally the notation \star is used to denote the Itô or Stratonovich dot according to the conditions described in the last section: τ_F and τ_{F2} are the decay time-scales for the one- and two-point functions of the fast dynamics respectively. This is then the main analytical result of our work, shown in eq. 3.

d. *Equilibrium: sanity check*

Now that we have the effective slow dynamics for general stochastic systems with time-scale separation, we want to check that in the equilibrium case, we recover the expected fluctuation-dissipation relation: $D_{ab}(x) = T \gamma_{ab}(x)$. Equilibrium in our original system will correspond to lack of any driving forces: thus all the forces must come from gradients of a single potential landscape $U(x_a, y_i)$: $F_a = -\partial_a U$ and $f_i = -\partial_i U$. Focusing on the expression for γ_{ab} above

we note that in this case $\partial_b f_i = -\partial_b \partial_i U = \partial_i F_b$

$$\gamma_{ab}(x, t) = \delta_{a,b} + \epsilon \int dt' (t - t') \langle i \tilde{y}_i \partial_i F_b |_{t'}, F_a |_t \rangle_{y|fix x}$$

We then note that the response field for the force F_b is given by $\tilde{F}_b = \tilde{y}_i \partial_i F_b$ when x is fixed, as it is here. Finally in MSR we know that $\langle i \tilde{F}_b, F_a \rangle$ gives the linear response function for F , and so by fluctuation-dissipation theorem $\langle i \tilde{F}_b |_{t'}, F_a |_t \rangle = \partial_{t'} \langle F_b |_{t'}, F_a |_t \rangle / T$ for $t' < t$ (zero otherwise). Using this in the above expression and integrating by parts:

$$\gamma_{ab}(x, t) = \delta_{a,b} + \frac{\epsilon}{2T} \int dt' \langle F_b |_{t'}, F_a |_t \rangle_{y|fix x}$$

$$= D_{ab}/T$$

(The factor of two dividing the integral comes from the fact that while the correlator is time-symmetric, the response function is causal.) We thus recover the desired result.

ACKNOWLEDGEMENTS: We are grateful to Jordan Horwitz, Tal Kachman, Robert Marsland, and David Theurel for provoking discussions and thoughtful comments on this article. P.V.C. and J.L.E. are supported by the Gordon and Betty Moore Foundation through Grant GBMF4343. J.L.E. further acknowledges the Cabot family for their generous support of Massachusetts Institute of Technology.

-
- [1] Jeremie Palacci, Stefano Sacanna, Asher Preska Steinberg, David J. Pine, and Paul M. Chaikin. Living crystals of light-activated colloidal surfers. *Science*, 339(6122):936–940, 2013.
- [2] Tim Sanchez, Daniel TN Chen, Stephen J DeCamp, Michael Heymann, and Zvonimir Dogic. Spontaneous motion in hierarchically assembled active matter. *Nature*, 491(7424):431–434, 2012.
- [3] Volker Schaller, Christoph Weber, Christine Semmrich, Erwin Frey, and Andreas R Bausch. Polar patterns of driven filaments. *Nature*, 467(7311):73–77, 2010.
- [4] Christopher Jarzynski. Nonequilibrium equality for free energy differences. *Physical Review Letters*, 78(14):2690, 1997.
- [5] Gavin E Crooks. Entropy production fluctuation theorem and the nonequilibrium work relation for free energy differences. *Physical Review E*, 60(3):2721, 1999.
- [6] Massimiliano Esposito and Christian Van den Broeck. Three detailed fluctuation theorems. *Physical review letters*, 104(9):090601, 2010.
- [7] Jeremy L England. Statistical physics of self-replication. *The Journal of chemical physics*, 139(12):09B623_1, 2013.
- [8] Robert Marsland III and Jeremy England. Far-from-equilibrium distribution from near-steady-state work fluctuations. *Physical Review E*, 92(5):052120, 2015.
- [9] Jorge Kurchan. Non-equilibrium work relations. *Journal of Statistical Mechanics: Theory and Experiment*, 2007(07):P07005, 2007.
- [10] Elias Putzig, Gabriel S Redner, Arvind Baskaran, and Aparna Baskaran. Instabilities, defects, and defect ordering in an overdamped active nematic. *Soft matter*, 12(17):3854–3859, 2016.
- [11] Cesare Nardini, Étienne Fodor, Elsen Tjhung, Frédéric van Wijland, Julien Tailleur, and Michael E Cates. Entropy production in field theories without time-reversal symmetry: quantifying the non-equilibrium character of active matter. *Physical Review X*, 7(2):021007, 2017.
- [12] Gabriel S Redner, Michael F Hagan, and Aparna Baskaran. Structure and dynamics of a phase-separating active colloidal fluid. *Physical review letters*, 110(5):055701, 2013.
- [13] AY Grosberg and J-F Joanny. Nonequilibrium statistical mechanics of mixtures of particles in contact with different thermostats. *Physical Review E*, 92(3):032118, 2015.
- [14] Nikolai Nikola, Alexandre P Solon, Yariv Kafri, Mehran Kardar, Julien Tailleur, and Raphaël Voituriez. Active particles with soft and curved walls: Equation of state, ratchets, and instabilities. *Physical Review Letters*, 117(9):098001, 2016.
- [15] Laurent Corte, PM Chaikin, Jerry P Gollub, and DJ Pine. Random organization in periodically driven systems. *Nature Physics*, 4(5):420–424, 2008.
- [16] MV Berry and JM Robbins. Chaotic classical and half-classical adiabatic reactions: geometric magnetism and deterministic friction. In *Proceedings of the Royal Society of London A: Mathematical, Physical and Engineering Sciences*, volume 442, pages 659–672. The Royal Society, 1993.
- [17] Christopher Jarzynski. Thermalization of a brownian particle via coupling to low-dimensional chaos. *Physical review letters*, 74(15):2937, 1995.
- [18] Eric Lutz. Fractional langevin equation. *Physical Review E*, 64(5):051106, 2001.
- [19] Patrick R Zulkowski, David A Sivak, Gavin E Crooks, and Michael R DeWeese. Geometry of thermodynamic control. *Physical Review E*, 86(4):041148, 2012.
- [20] Patrick R Zulkowski, David A Sivak, and Michael R DeWeese. Optimal control of transitions between nonequilibrium steady states. *PloS one*, 8(12):e82754, 2013.
- [21] Benjamin B Machta. Dissipation bound for thermodynamic control. *Physical review letters*, 115(26):260603, 2015.
- [22] Luca DAlessio, Yariv Kafri, and Anatoli Polkovnikov. Negative mass corrections in a dissipative stochastic environment. *Journal of Statistical Mechanics: Theory and Experiment*, 2016(2):023105, 2016.
- [23] Christian Maes and Stefano Steffenoni. Friction and noise for a probe in a nonequilibrium fluid. *Physical Review E*, 91(2):022128, 2015.
- [24] Urna Basu, Christian Maes, and Karel Netočný. Statistical forces from close-to-equilibrium media. *New Journal of Physics*, 17(11):115006, 2015.
- [25] Crispin W Gardiner. *Handbook of stochastic methods for physics, chemistry and the natural sciences, vol. 13 of.* 1985.
- [26] Lin-Yuan Chen, Nigel Goldenfeld, and Yoshitsugu Oono. Renormalization group and singular perturbations: Multiple scales, boundary layers, and reductive perturbation theory. *Physical Review E*, 54(1):376, 1996.
- [27] Richard Phillips Feynman and Frank Lee Vernon. The theory of a general quantum system interacting with a linear dissipative system. *Annals of physics*, 24:118–173, 1963.
- [28] Eric Lutz. Fractional transport equations for lévy stable processes. *Physical review letters*, 86(11):2208, 2001.
- [29] J. Cardy, G. Falkovich, K. Gawedzki, S. Nazarenko, and O.V. Zaboronski. *Non-equilibrium Statistical Mechanics and Turbulence.* London Mathematical Society Le. Cambridge University Press, 2008.
- [30] Igor Tikhonenkov, Amichay Vardi, James R Anglin, and Doron Cohen. Minimal fokker-planck theory for the thermalization of mesoscopic subsystems. *Physical review letters*, 110(5):050401, 2013.
- [31] Mehran Kardar. *Statistical physics of fields.* Cambridge University Press, 2007.

- [32] Ole Peters and William Klein. Ergodicity breaking in geometric brownian motion. *Physical review letters*, 110(10):100603, 2013.
- [33] Ulrike Feudel, Celso Grebogi, Brian R Hunt, and James A Yorke. Map with more than 100 coexisting low-period periodic attractors. *Physical Review E*, 54(1):71, 1996.
- [34] Suso Kraut, Ulrike Feudel, and Celso Grebogi. Preference of attractors in noisy multistable systems. *Physical Review E*, 59(5):5253, 1999.
- [35] Jordan M Horowitz, Kevin Zhou, and Jeremy L England. Minimum energetic cost to maintain a target nonequilibrium state. *Physical Review E*, 95(4):042102, 2017.
- [36] Matthew J Todd, George H Lorimer, and D Thirumalai. Chaperonin-facilitated protein folding: optimization of rate and yield by an iterative annealing mechanism. *Proceedings of the National Academy of Sciences*, 93(9):4030–4035, 1996.
- [37] Jakub Spiechowicz, Marcin Kostur, and Jerzy Łuczka. Brownian ratchets: How stronger thermal noise can reduce diffusion. *Chaos: An Interdisciplinary Journal of Nonlinear Science*, 27(2):023111, 2017.
-

SUPPLEMENTARY MATERIALS: KICKED ROTOR ON A CART CORRELATORS

In this addendum we present the analytical calculations required to make the predictions for the Kicked Rotor on a cart toy model described in the main text. For convenience, we reproduce the dimensionless equations of motion here (this time including the direct effect of kicks on the cart in F_x):

$$\begin{aligned}
 \dot{\theta} &= \underbrace{v}_{\equiv f_\theta} \\
 \dot{v} &= \underbrace{-K(x) \sin \theta \delta(t-n) - \ddot{x} \cos \theta - bv + \sqrt{2Tb} \xi}_{\equiv f_v} \\
 c\dot{x} &= -\partial_x U(x) + \underbrace{\sin \theta (v^2 + K(x) \cos \theta \delta(t-n) - \ddot{x} \sin \theta)}_{\equiv F_x} + \sqrt{2Tc} \xi
 \end{aligned} \tag{S.1}$$

The units were chosen such that rotor arm length, mass, and kicking period are all =1. The part in black gives simple kicked rotor dynamics, red part weakly (for $b \ll 1$) couples it to a thermal bath at temperature T , and blue part gives the coupling and dynamics of the cart. We assume throughout that the bath temperature here is very low $T \sim 0$ to highlight the effect of the chaotic fluctuations of kicked rotor. Strong time-scale separation, which here is achieved by assuming $c \gg 1$, implies that terms $\propto \ddot{x}$ will be small. To see when precisely we can be justified in dropping these, we estimate their magnitude for the two regimes: the forced regime (“during the kick”) and the free rotation. For the forced regime, since $\delta(t)$ is a distribution, we can only talk about the integrals

$$\begin{aligned}
 \delta v_K &= \lim_{\eta \rightarrow 0} \int_{-\eta}^{+\eta} dt \dot{v} = -K \sin \theta - \cos \theta [\dot{x}]_{-\eta}^{+\eta} = -K \sin \theta - \frac{K}{c} \sin^2 \theta \cos \theta [K \sin \theta - 2v] \\
 \delta x_K &= \lim_{\eta \rightarrow 0} \int_{-\eta}^{+\eta} dt \dot{x} = K \sin \theta \cos \theta - \frac{K}{c} \sin^4 \theta [K \sin \theta - 2v]
 \end{aligned}$$

For the free rotation, we can simply differentiate the unforced part of the last line in eq. S.1 with respect to time, which gives $c\ddot{x} = v^3 \cos \theta$ to leading order. Thus, to ignore the \ddot{x} terms, we need $Kv/c \ll K$ for the driven regime, and $v^3/c \ll bv$ for free rotation. While the former condition is easy to satisfy for a large c , the latter one competes with our additional assumption that $b \ll 1$ and can be difficult to satisfy numerically, especially as velocities v can sometimes get very large – thus we will keep the $\ddot{x} \sin \theta$ term as an additional perturbative correction to the free dynamics.

e. Chaotic Kicked Rotor steady-state

To proceed in evaluating the different terms in the expression for the effective slow dynamics (eq.3 in main text), we need to find the steady-state distribution over (θ, v) for a fixed cart position x . As mentioned in the main text, for strong driving $K \gtrsim 5$, the kicked rotor dynamics are fully chaotic, and thus the steady-state thermalizes all input energy. This immediately implies that the probability distribution is of form $p_{ss}(\theta, v | x) \propto \exp\left[-\frac{v^2}{2T_R(x)}\right]$ – uniform over θ and Gaussian over v , parametrised by a single number $T_R(x)$ – effective rotor temperature. The symmetries of this distribution guarantee that $\langle F_x \rangle_{ss} = 0$.

To find this temperature, we can use the argument from eq. 5 of the main text, which tells us that this steady-state will have a dissipation rate:

$$\delta Q = \int dt v \circ \left(bv - \sqrt{2T_0 b} \xi \right) = b \left(\langle v^2 \rangle - \sqrt{2T_0 b} \left\langle \frac{v_{t+\delta t} + v_t}{2} \xi_t \right\rangle \right) \delta t$$

where for underdamped, forced Langevin dynamics, we have in general:

$v_{t+\delta t} = v_t + \delta t (-bv_t + F(x, v, t) + \sqrt{2T_0 b} \xi)$. Thus, while v_t is completely uncorrelated with ξ_t : $\langle v_t \xi_t \rangle = 0$, $v_{t+\delta t}$ is correlated only via the thermal noise term: $\langle v_{t+\delta t} \xi_t \rangle = \sqrt{2T_0 b}$, and is independent of any interaction

or driving forces $F(x, v, t)$. This gives, for mass=1:

$$\mathcal{P} \equiv \frac{\partial Q}{\partial t} = b (T_{eff} - T_0). \quad (\text{S.2})$$

(note that if v were a vector in d -dimensions, we would multiply this expression by d). With this, and neglecting the bath temperature T_0 , we can balance the work flow in and heat flow out per kick, to get:

$$\begin{aligned} 0 = \delta W - \delta Q &= \left\langle \lim_{\eta \rightarrow 0} \int_{-\eta}^{+\eta} dt v \circ (-K \sin \theta) \right\rangle_{ss} - b \langle v^2 \rangle_{ss} = \left\langle \left(v_{pre} - \frac{K}{2} \sin \theta \right) (-K \sin \theta) \right\rangle_{ss} - b T_R \\ \Rightarrow T_R &= \frac{K^2}{4b} \end{aligned}$$

where v_{pre} is the pre-kick velocity, which is uncorrelated with θ . Since this gives the variance of typical rotor velocities, we can use it to simplify the time-scale separation condition derived above $v^3/c \ll b v$ down to $K/c \ll b^2$ – which is quite difficult to satisfy in addition to $b \ll 1$. Thus, while this result is correct, it turns out that $O[1/c]$ correction coming from the cart coupling term $\ddot{x} \cos \theta$ is very important here. Note that eq. 3 in main text tells us to include x -dependence of the steady-state in correcting the effective damping coefficient γ , however as this term depends only on \ddot{x} and not x itself, the steady-state does not gain any x -dependence from it, but rather an x -uniform correction which must be included directly. In this case, as the dynamics are still chaotic and distribution thermal, while the work extracted from the drive δW is not affected (since any work done on the overdamped cart is immediately dissipated and so can be ignored), so the coupling to cart simply adds another channel for heat dissipation:

$$\begin{aligned} \delta Q &= b \langle v^2 \rangle_{ss} + \left\langle \int_0^1 dt c \dot{x}^2 \right\rangle_{ss} = b T_R + \frac{1}{c} \int_0^1 dt \langle F_x |_t F_x |_t \rangle_{ss} \\ &= b T_R + \frac{1}{c} \left[\int_0^1 dt \langle (v^2 \sin \theta)^2 \rangle_{ss} + \langle 2 K v^2 \sin^2 \theta \cos \theta |_{t=0} \rangle_{ss} \right] \\ &= b T_R + \frac{1}{c} \left[\frac{3}{2} T_R^2 + 0 \right] \\ \Rightarrow T_R &= \frac{bc}{3} \left(\sqrt{1 + \frac{3K^2}{2b^2c}} - 1 \right) < \frac{K^2}{4b} \end{aligned}$$

where we assumed that v and θ are uncorrelated during most of the time $0 < t < 1$, as justified below. This correction significantly lowers the typical velocities and well reproduced in the results of the simulations for large, but practical values of c (e.g., for $b = 10^{-2}$, $c = 10^4$, $K = 10 \Rightarrow T_R \approx 375 < K^2/4b = 2500$, or for $b = 10^{-1}$, $c = 5 \times 10^4$, $K = 10 \Rightarrow T_R \approx 230 < K^2/4b = 250$).

f. Damping and Noise correction

With the above understanding of the steady-state, we now proceed to compute the two-time correlations functions needed to get the corrections on the slow dynamics given by eq.3 of the main text. We begin by noting their general structure here: each kick introduces correlations between θ and v , after which, while v remain approximately constant until the next kick (for $b \ll 1$), θ spins around and correlations decay. The typical decay time-scale in this system can be estimated by looking at the decay:

$$\langle \sin \theta(0) \sin \theta(t) \rangle_{ss} = \langle \sin \theta(0) \sin (\theta(0) + vt) \rangle_{ss} = \frac{1}{2} - \frac{T_R}{4} t^2 + O[t^4]$$

where we assume θ and v to be uncorrelated over the time-window. This gives decay $\tau \sim 1/\sqrt{T_R}$, which for typical values of parameters (e.g., for $b = 10^{-1}$, $c = 5 \times 10^4$, $K = 10$) could be around $1/20$. The key here is that in most cases the decay time is much shorter than 1 (the kicking period). Figure S.1 shows numerical results for $\langle F_x(t), F_x(t') \rangle$ correlation in the chaotic phase to give a sense of how these quantities typically look for the given system. Since the $\theta - v$ correlations are only generated by kicks, this implies that most of

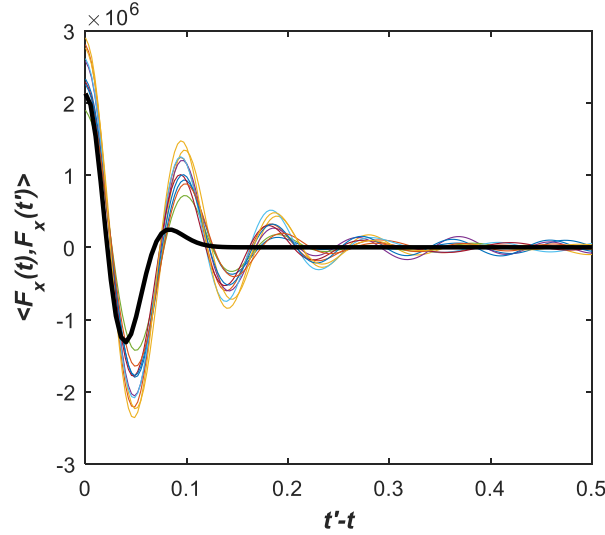


FIG. S.1: decay of the $\langle F_x |_t, F_x |_{t'} \rangle_{(\theta, v) | fix x}$ correlator over time after a kick at 0 (kick period =1). Colored curves – different numerical realizations, black curve – analytical prediction.

the time they are uncorrelated – as we have assumed a few times above. Moreover, this means that our noise and damping corrections should always be interpreted as Itô for this system, as discussed in the Appendix b of the main text.

Using this result we can immediately see that the damping correction vanishes (see eq.S.1 for definitions of f_θ, f_v):

$$\begin{aligned} \delta\gamma &= \frac{1}{c} \int dt' (t-t') \left\langle i \left(\tilde{\theta} \partial_x f_\theta + \tilde{v} \partial_x f_v \right) |_{t'}, F_x |_t \right\rangle_{(\theta, v) | fix x} \\ &= \frac{1}{c} \int dt' (t-t') \left\langle -i \tilde{v} K'(x) \sin \theta \sum_n \delta(t' - n) |_{t'}, F_x |_t \right\rangle_{(\theta, v) | fix x} \\ &= \frac{1}{c} \sum_n (t-n) \langle -i \tilde{v} K'(x) \sin \theta |_n, F_x |_t \rangle_{(\theta, v) | fix x} = 0 \end{aligned}$$

as the correlator vanishes by the symmetries of the thermal steady-state.

With that, to find the effective temperature experienced by the cart, we need only compute the noise correction, as: $T_{eff} = \frac{1}{2c} \int dt' \langle F_x |_{t'}, F_x |_t \rangle_{(\theta, v) | fix x}$. From eq.S.1, we get $F_x = v^2 \sin \theta + K(x) \sin \theta \cos \theta \delta(t-n) - \ddot{x} \sin^2 \theta = (\text{centripetal } F_c) + (\text{direct kick coupling } F_k) - (\text{inertia } F_i)$. Unlike in f_v , where the term bv was comparable magnitude to $\ddot{x} \cos \theta$, here F_c and F_k are both $> O[1]$, and thus the inertia F_i is distinctly sub-leading and can be dropped. We now proceed to individually compute the $\langle F_c, F_c \rangle$, $\langle F_k, F_k \rangle$, $\langle F_c, F_k \rangle = \langle F_k, F_c \rangle$ contributions.

For the $\langle F_c, F_c \rangle$ term, we see that far from the kicks, where θ and v are uncorrelated, we get:

$$\int dt' \langle v^2 \sin(\theta + t'v), v^2 \sin \theta \rangle_{(\theta, v) | fix x} = 0$$

which can be evaluated analytically in Mathematica. The leading correction to this quantity then comes from the $\theta - v$ correlations generated by the kicks. To capture these, we write all velocities and angles in

terms of their values before the last kick – at a time when they were guaranteed to be uncorrelated. Thus

$$v(t) = \begin{cases} v_{pre} & \\ v_{pre} - K \sin \theta_{pre} & \end{cases} \quad \text{and} \quad \theta(t) = \begin{cases} \theta_{pre} + t v_{pre} & t < 0 \\ \theta_{pre} + t (v_{pre} - K \sin \theta_{pre}) & t > 0 \end{cases}$$

Using these expressions, we can thus evaluate $\iint dt dt' \langle F_c |_{t'} , F_c |_t \rangle$ piecewise (where a second integral must be included since the time-translation-invariance is now broken). Dropping the subscript *pre*, we have:

$$\begin{aligned} & \int_{-1/2}^{1/2} dt \int_{-\infty}^{\infty} dt' \langle v(t)^2 \sin \theta(t), v(t')^2 \sin \theta(t') \rangle_{(\theta,v)|fix x} \\ &= \begin{cases} \left\langle \int_0^{1/2} dt \int_0^{\infty} dt' (v - K \sin \theta)^4 \sin(\theta + t(v - K \sin \theta)) \sin(\theta + t'(v - K \sin \theta)) \right\rangle_{(\theta,v)|fix x} \\ + 2 \left\langle \int_{-1/2}^0 dt \int_0^{\infty} dt' v^2 \sin(\theta + tv) (v - K \sin \theta)^2 \sin(\theta + t'(v - K \sin \theta)) \right\rangle_{(\theta,v)|fix x} \\ + \left\langle \int_{-1/2}^0 dt \int_{-\infty}^0 dt' v^4 \sin(\theta + tv) \sin(\theta + t'v) \right\rangle_{(\theta,v)|fix x} \end{cases} \\ &= \begin{cases} K^2/8 + T_R/2 \\ -T_R \\ +T_R/2 \end{cases} = K^2/8 \end{aligned}$$

where all integrals can be evaluated analytically (in Mathematica) if we take the time integrals first, and then average over the (uncorrelated) θ and v . The analytical expression for the two-time correlator thus obtained is compared to numerical results in fig.S.1. Similarly for the other terms:

$$\begin{aligned} & \int dt' \langle F_k |_{t'} , F_k |_t \rangle_{(\theta,v)|fix x} = \left\langle \int_{-\infty}^{\infty} dt' \int_{-1/2}^{1/2} dt \sum_{n,m} \frac{K}{2} \sin 2\theta(t) \delta(t-n) \frac{K}{2} \sin 2\theta(t') \delta(t'-m) \right\rangle_{(\theta,v)|fix x} \\ &= \sum_m \frac{K^2}{4} \langle \sin 2\theta(0) \sin 2\theta(m) \rangle_{(\theta,v)|fix x} = K^2/8 \end{aligned}$$

$$\begin{aligned} & \int_{-\infty}^{\infty} dt' \langle F_k |_{t'} , F_c |_t \rangle_{(\theta,v)|fix x} = \int_0^{\infty} dt' \left\langle \frac{K}{2} \sin 2\theta (v - K \sin \theta)^2 \sin(\theta + t'(v - K \sin \theta)) \right\rangle_{(\theta,v)|fix x} \\ &= -K^2/8 = \int_{-\infty}^{\infty} dt' \langle F_c |_t , F_k |_{t'} \rangle_{(\theta,v)|fix x} \end{aligned}$$

Adding up all four terms, we thus get $T_{eff} = \frac{1}{2c} \int dt' \langle F_x |_{t'} , F_x |_t \rangle_{(\theta,v)|fix x} = 0$. Here we clearly see that the cancellation comes up due to the anti-correlations between the centripetal force and the kick coupling. In this particular case, the cancellation is somewhat accidental, and is a consequence of the simplicity of the system – the functional form of couplings is quite restricted. In general, we expect such cancellations to be unlikely in higher-dimensional systems. As discussed in the main text, to make the system interesting and get a finite T_{eff} , we can simply eliminate the direct kick-cart coupling F_k from the dynamics altogether, with the physical interpretation of “pinning” down the cart at the instant of the kick. This leaves only F_c , thus giving $T_{eff} = K^2/16c$, as desired.

Note also that the rotor temperature T_R calculated above ends up dropping out and does not affect any of the time-integrated correlators, but only the particulars of their time-dependence as $\langle F_x(t), F_x(t') \rangle_{(\theta,v)|fix x}$. Thus the only really key role it played for us was to show that these correlators decay faster than kicking period.

g. Ordered KR steady-state

On the other hand for weak driving $K \lesssim 5$, the kicked rotor undergoes dynamic regularization, and in steady-state is found in one of the integrable attractors in its phase space. Thus, none of the above arguments apply here. Instead, the main regular regions correspond to the rotor completing n full revolutions per kick, with $n = \dots, -2, -1, 0, 1, 2, \dots$. As it does, there are no stochastic fluctuations, other than those from the thermal bath, and as the steady-state lacks the symmetries of the thermal state, $\langle F_x \rangle_{ss} \neq 0$ except at $n = 0$. In fact, depending on the attractor that the rotor falls into, it will exert a persistent force on the cart, causing constant directed drift. We can easily estimate this drift force for the n 'th attractor as (here we again assume that $b \sim O[1/c] \ll 1$, and let $v_n \equiv 2\pi n$):

$$\langle F_x \rangle_{ss} = \int_0^1 dt v^2(t) \sin \theta(t) = b v_n + \frac{v_n^3}{2c} + O[b^2]$$

$$\text{where } v(t) = 2\pi n - b v t - \frac{1}{c} \int_0^t d\tau v^3 \cos^2(v\tau) + O[b^2] \quad \text{and} \quad \theta(t) = \int_0^t d\tau v(\tau)$$

where $v(t)$ dynamics are found by directly integrating eq.S.1 to first order in small parameters. However, as it is impossible to predict which of the attractors will be chosen, we can't a-priori tell the direction or speed that the cart will be moving at – though the options are restricted to the above small discrete set of possibilities parametrized by n .